

Supporting information

Synthesis, characterization and catalytic epoxidation property of a new tellurotungstate(IV)-supported rhenium carbonyl derivative

Jingkun Lu, Xinyi Ma, Baijie Xu, Peipei He, Pengtao Ma, Jingyang Niu* and Jingping Wang*

Henan Key Laboratory of Polyoxometalate Chemistry, Institute of Molecular and Crystal Engineering, College of Chemistry and Chemical Engineering, Henan University, Kaifeng, Henan 475004 P.R. China

E-mail address: jyniu@henu.edu.cn, jpwang@henu.edu.cn

Fax: (+86)371-23886876.

CONTENTS

Section 1 The bond valence sum calculations

Section 2 Selected bond lengths and angles

Section 3 Additional structural figures

Section 4 Additional measurements

Section 5 Catalytic properties

Section 1 The bond valence sum calculations

Table S1 The BVS calculations of Te and W atoms in polyoxoanion.

Atoms	BVS	Atoms	BVS
W1	6.241	W6	6.173
W2	6.193	W7	6.181
W3	6.164	W8	6.177
W4	6.240	W9	6.189
W5	6.307	W10	6.475
Te1	3.964		

Table S2 The BVS calculations of all oxygen atoms in polyoxoanion.

Atoms	BVS	Atoms	BVS
O1	1.841	O20	2.013
O2	1.841	O21	1.989
O3	1.995	O22	2.268
O4	1.835	O23	2.066
O5	1.762	O24	1.962
O6	2.272	O25	2.196
O7	1.849	O26	2.347
O8	1.741	O27	1.918
O9	1.715	O28	1.975
O10	1.969	O29	2.033
O11	2.000	O30	2.009
O12	2.051	O31	1.899
O13	1.991	O32	2.180
O14	2.147	O33	1.851
O15	1.982	O34	2.043
O16	1.871	O35	1.416
O17	2.134	O36	1.867
O18	2.051	O37	1.610
O19	1.944	O38	1.987

Section 2 Selected bond lengths and angles

Table S3 Selected bond length (Å) and bond angle (°) of compound **1**

Bonds	Length(Å)	Bonds	Angle(°)
Re-C(1)	1.88(2)	C(1)-Re-O(6)	93.1(8)
Re-C(2)	1.86(2)	C(1)-Re-O(16)	176.6(8)
Re-C(3)	1.91(2)	C(1)-Re-O(23)	101.5(8)
Re-O(6)	2.144(14)	O(6)-Re-O(16)	83.6(5)
Re-O(16)	2.148(13)	O(6)-Re-O(23)	83.4(6)
Re-O(23)	2.163(14)	O(16)-Re- O(23)	77.1(6)
Te-O(14)	1.899(12)	O(22)-Te-O(14)	90.7(6)
Te-O(22)	1.859(13)	O(22)-Te-O(32)	92.8(6)
Te-O(32)	1.873(13)	O(32)-Te-O(14)	93.9(5)
C(1)-O(36)	1.15(3)		
C(2)-O(37)	1.18(3)		
C(3)-O(38)	1.13(3)		

Section 3 Additional structural figures

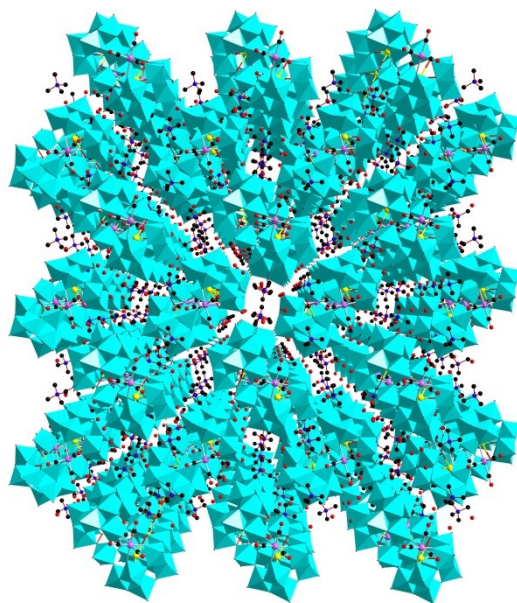


Figure S1. Packing diagram of **1** viewed along the a axis; Color code: Te, yellow; W, blue; Re, purple; C, black; O, red; WO₆, cyan.

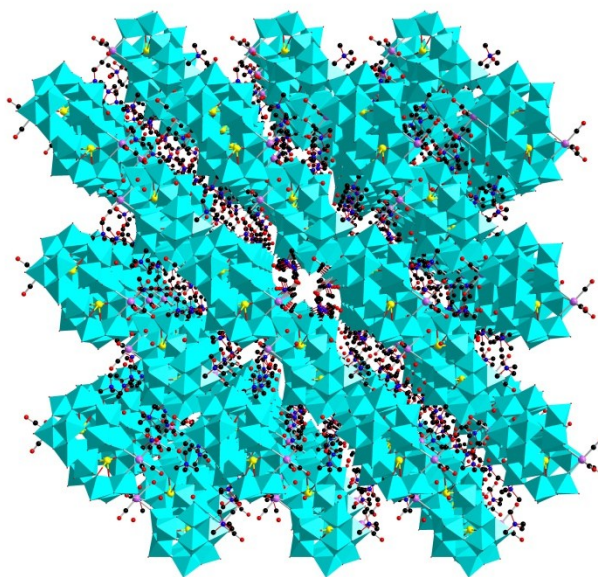


Figure S2. Packing diagram of **1** viewed along the b axis; Color code: Te, yellow; W, blue; Re, purple; C, black; O, red; WO₆, cyan.

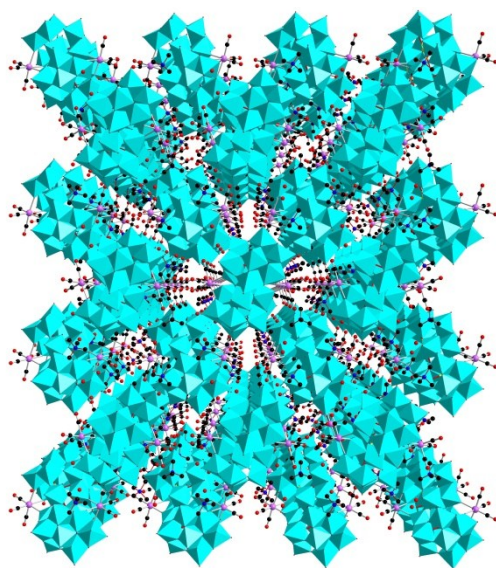


Figure S3. Packing diagram of **1** viewed along the *c* axis; Color code: Te, yellow; W, blue; Re, purple; C, black; O, red; WO₆, cyan.

Section 4 Additional measurements

4.1 IR Spectrum

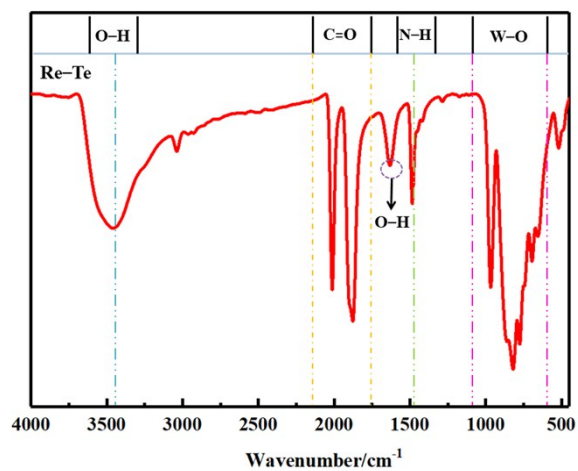


Figure S4. The IR spectrum of compound 1

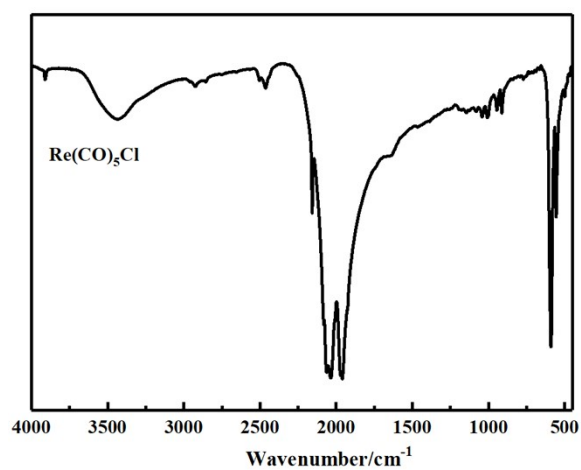


Figure S5. The IR spectrum of Re(CO)₅Cl

4.2 X-ray powder patterns

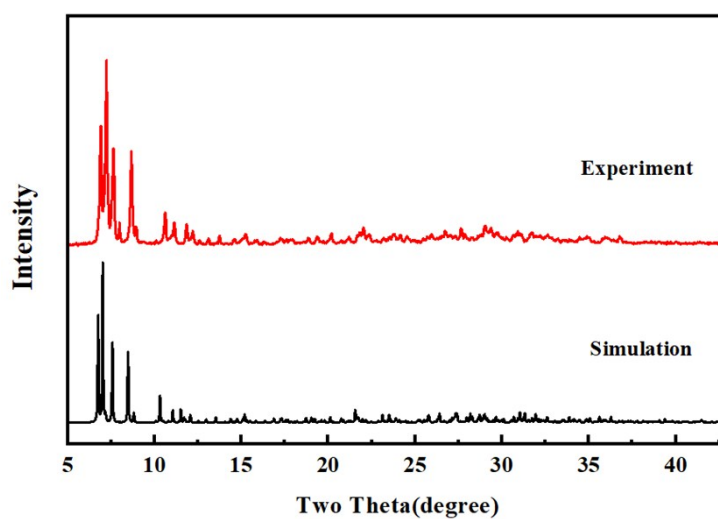


Fig. S6 The XPRD patterns for experiment (top) and simulated (bottom) of 1.

4.3 Thermogravimetric analysis

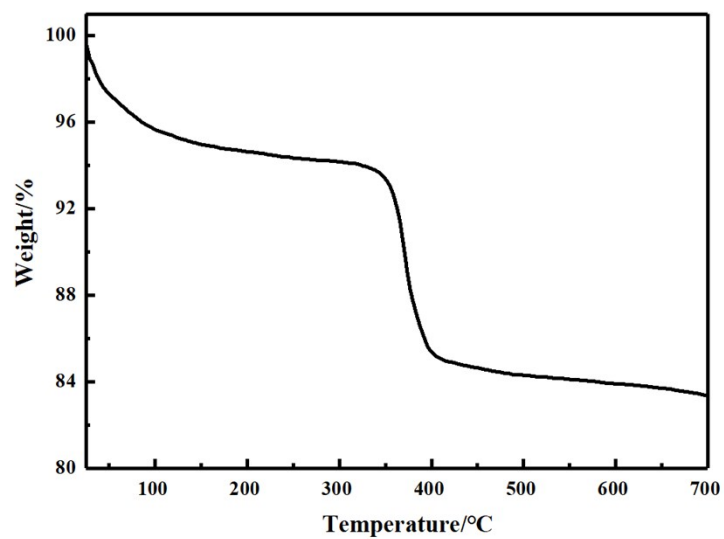


Fig. S7 Thermogravimetric curve of **1**.

4.4 UV-vis spectrum

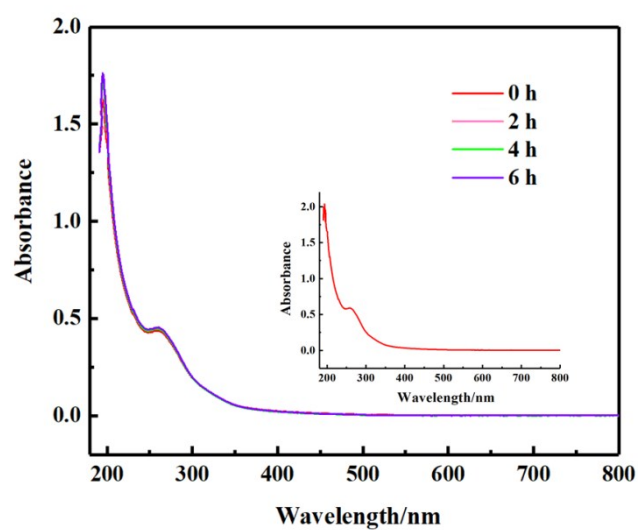



Figure S8. The UV-vis spectrum of **1** ($5 \times 10^{-5} \text{ mol}\cdot\text{L}^{-1}$)

Section 5 Catalytic properties

Table S4 Oxidation of cis-cyclooctene with different catalysts ^a

Entry	Substrate	Catalyst	Con. ^b (%) ^c	Sel. (%)
1		–	2.9	>99
2		Re(CO) ₅ Cl	3.4	>99
3		Na ₂ WO ₄ ·2H ₂ O	3.2	>99
4		Na ₂ TeO ₃	5.0	>99
5		Catalyst 1	98.2	>99
6		(NH ₄) ₈ {[Te ₂ Mo ₁₂ (OH)O ₄₄][Re(CO) ₃]}·13H ₂ O	6.3	>99

^a Reaction conditions: substrate (1 mmol), catalyst **1** (0.5 mol%), and H₂O₂ (3.0 mmol) were mixed in 5 mL acetonitrile at 75 °C. Unless otherwise noted. ^b Determined by GC analyses based on initial substrate.

We have checked the rate of H₂O₂ decomposition in the presence of catalyst without any organic substrate. The concentration of the H₂O₂ solution was determined by volumetric titration using a standard solution of potassium permanganate (0.1 M). The ln(C_t/C₀) values are plotted against the reaction time in Fig. 5. C₀ and C_t are the initial H₂O₂ concentration and the H₂O₂ concentration at time t, respectively. The linear fit of the data reveals that the decomposition process follows pseudo-first-order kinetics for the H₂O₂ decomposition (R² = 0.998). By using Equations (1) (–dC_t/d_t = kC_t) and (2) (ln C₀/C_t = kt), the observed rate constant k for the H₂O₂ decomposition was determined to be –0.016 min^{–1}.

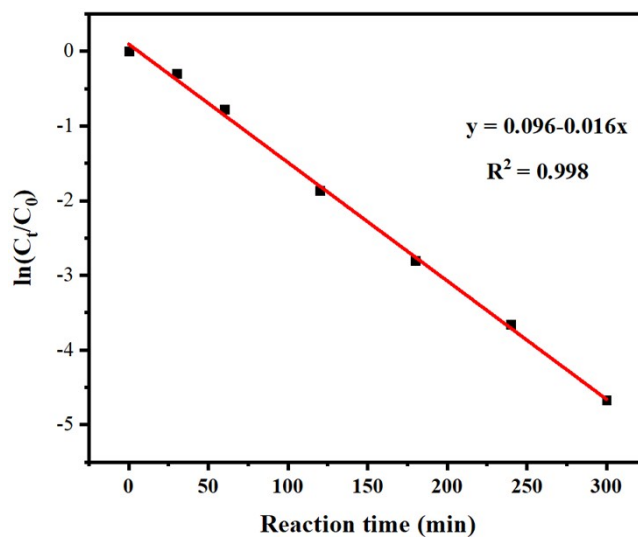


Figure S9. Kinetic profiles of the H₂O₂ decomposition reaction.

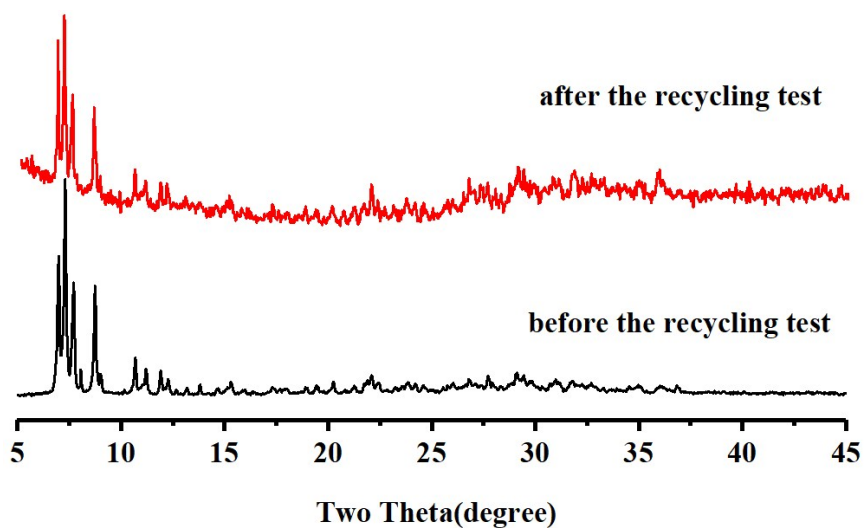


Figure S10. The XRPD of **1** before and after the recycling tests

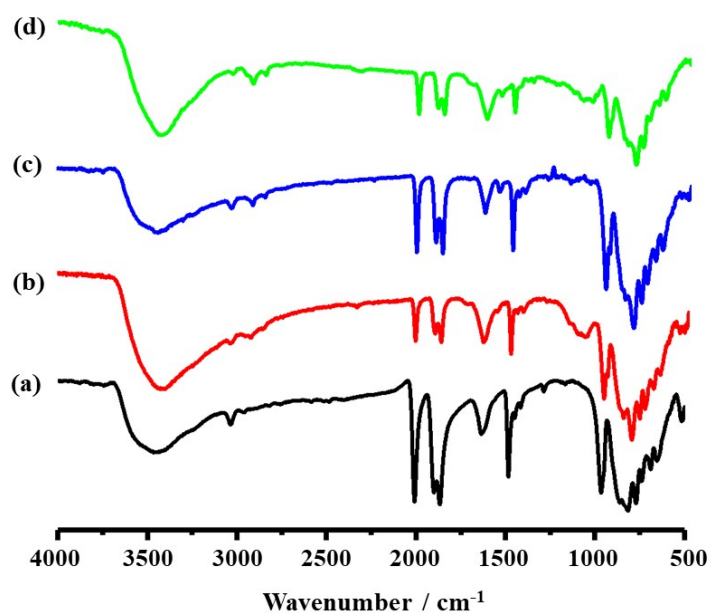
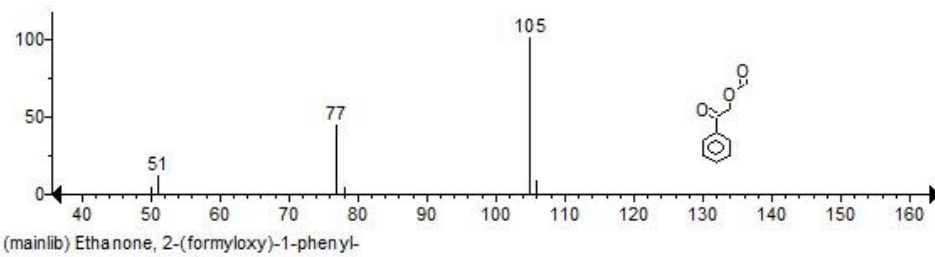
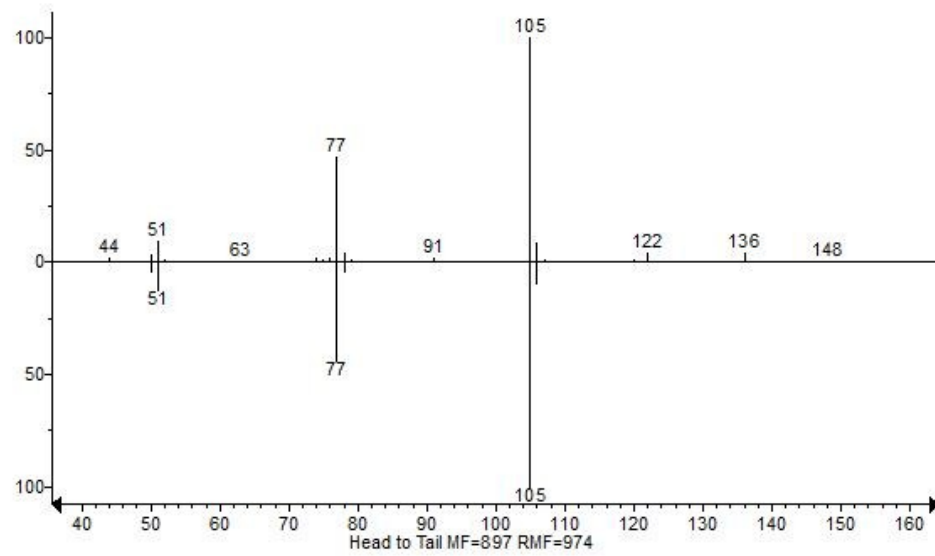
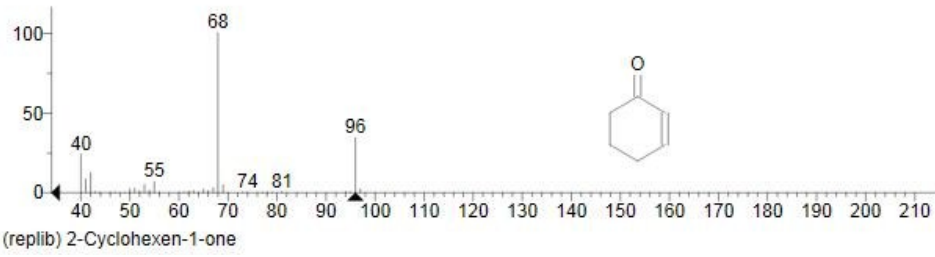
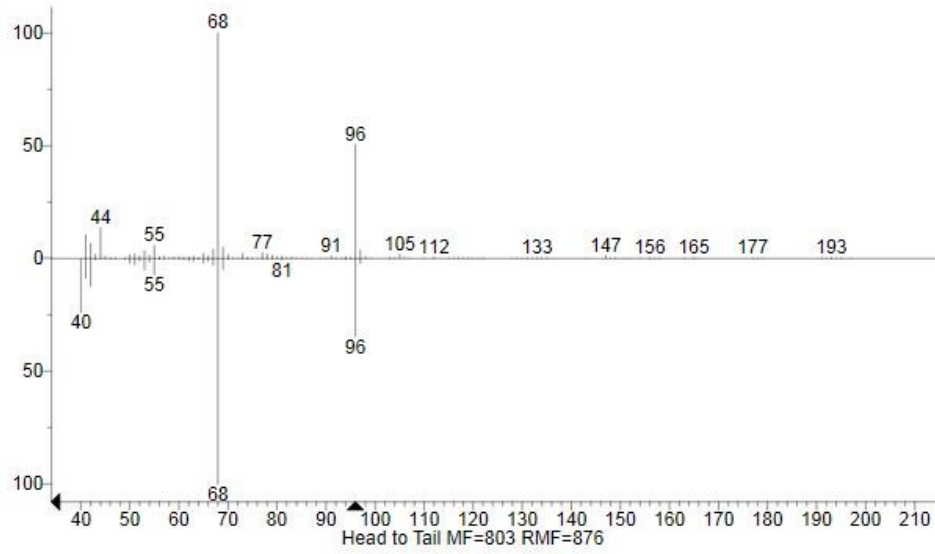
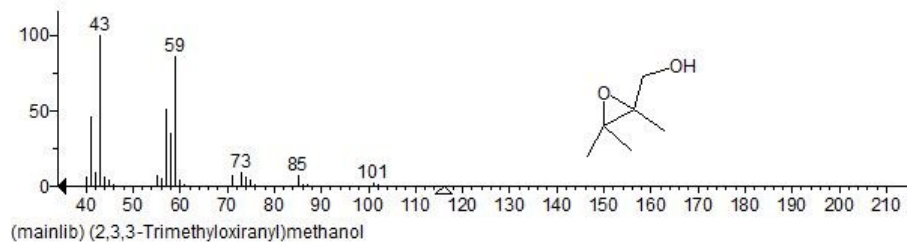
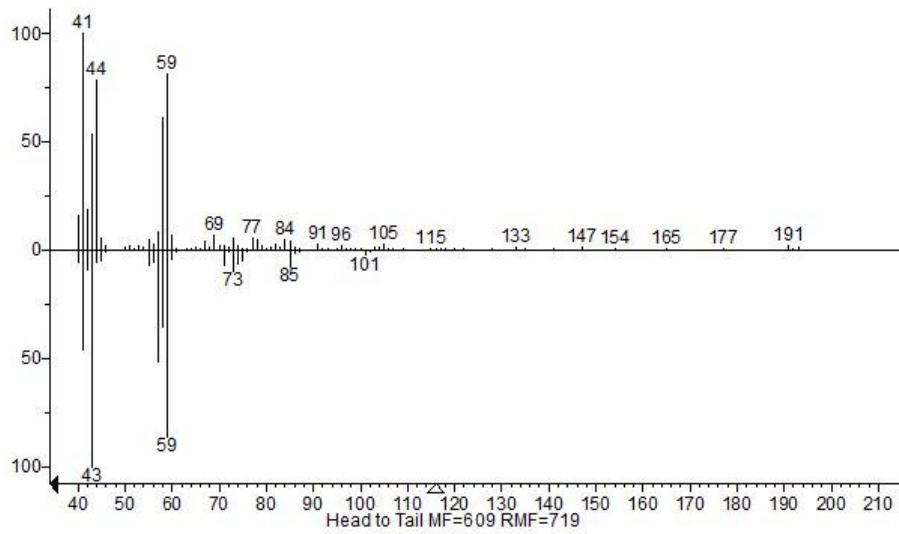
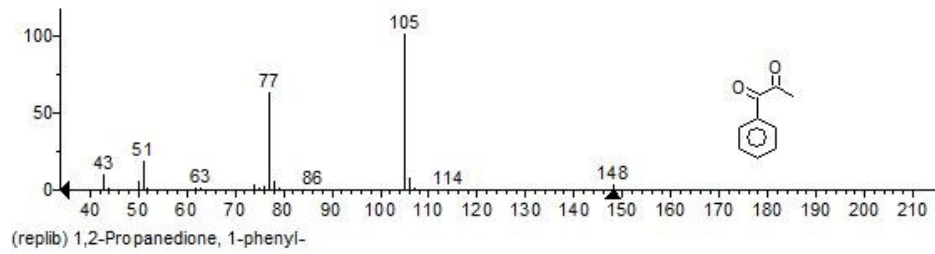
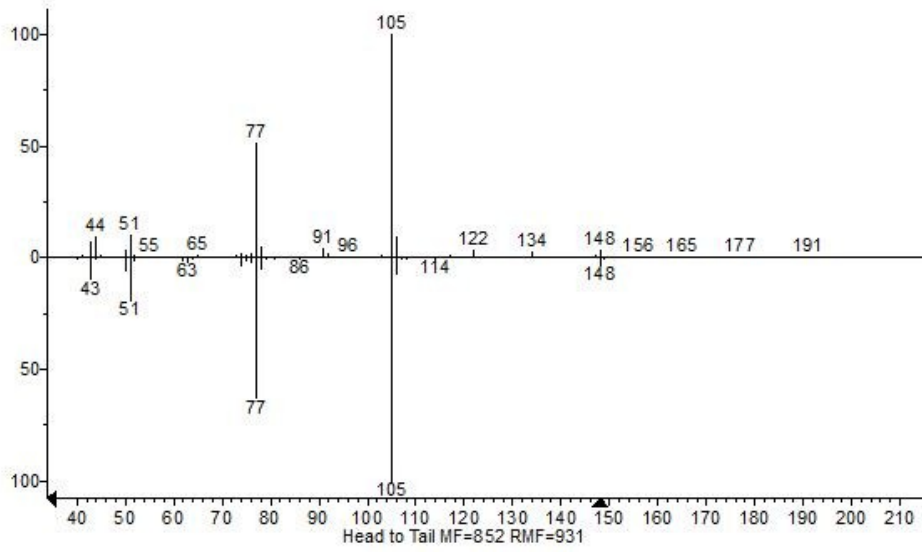


Figure S11. IR spectra of catalyst **1** before and after the recycling tests; (a) IR spectrum of catalyst **1**; (b) IR spectrum of the sample tested 1st run; (c) IR spectrum of the sample tested 2nd run; (d) IR spectrum of the sample tested 3rd run.





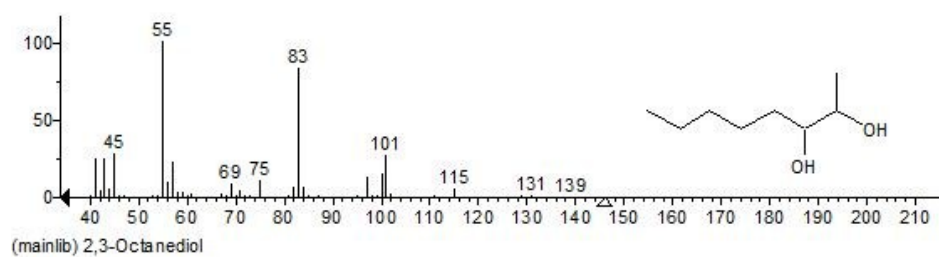
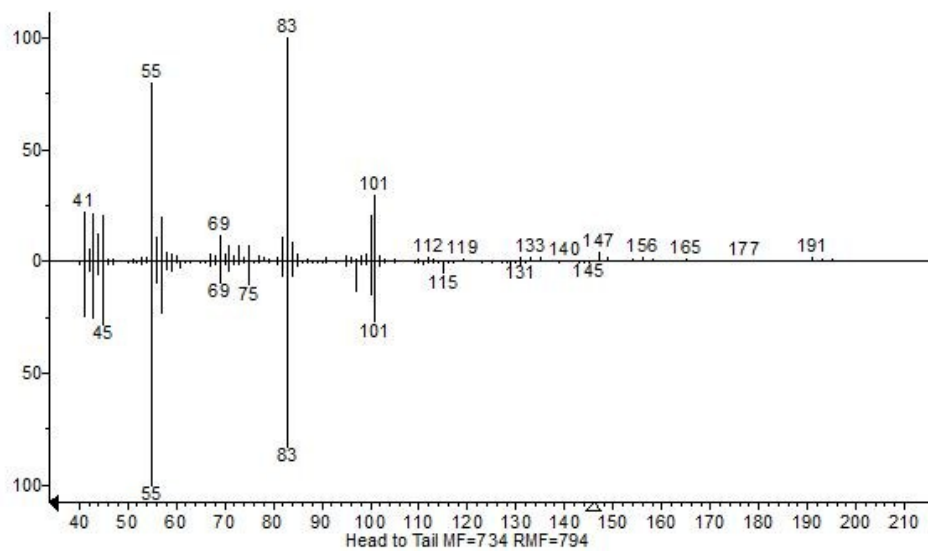


Figure S12. Mass spectra of the side products of entries 2, 4, 7, 8 and 10 in Table 4